JOURNAL OF SOLID STATE CHEMISTRY 33, 335–339 (1980)

# Paramagnetic Defects in $\alpha$-$W_xV_2O_5$

JACQUES LIVAGE, CHAKIB R'KHA, AND DOMINIQUE BALLUTAUD
*Spectrochimie du Solide, ERA 387, Université Paris VI, 4, place Jussieu, Paris 5e, France*

AND JEAN-CLAUDE GRENET
*Chimie Appliquée, Bâtiment 414, Université Paris XI, 91405 Orsay, France*

Received February 21, 1979; in revised form October 10, 1979

Paramagnetic defects in $\alpha$-$W_xV_2O_5$ have been studied by ESR. A model is proposed where the unpaired electron arising from a valence induction effect remains localized on a single vanadium ion near the $W^{6+}$ along the *b* direction. Introducing $W^{6+}$ leads to a lattice distortion which is more important than that in the case of $Mo^{6+}$. A slight displacement of vanadium along the *a* direction is observed in the defect, $V^{4+}$ showing a stronger tendency toward octahedral coordination than $V^{5+}$.

## Introduction

Nonstoichiometric vanadium pentoxide $V_2O_5$ is a low-mobility *n*-type semiconductor. Its properties arise from the hopping of an unpaired electron between $V^{4+}$ and $V^{5+}$ ions (*1–3*). At low temperature, the charge carriers are trapped on defects and the unpaired electron is delocalized over two vanadium ions separated by an oxygen vacancy (*4*). The nature of these defects may be modified by doping the oxide. In $\alpha$-$M_xV_2O_5$ bronzes ($M = Li^+, Na^+$), for instance the electron is delocalized over the four equivalent vanadium ions surrounding the interstitial monovalent impurity (*5*, *6*).

$MoO_3$ and $WO_3$ give extended solid solutions with $V_2O_5$ (*7*, *8*). These solid solutions have the same orthorhombic structure as $V_2O_5$, the hexavalent ion $M^{6+}$ occupying vanadium lattice sites. Such systems have been extensively studied (*9–12*). NMR experiments (*13*) show that introducing $M^{6+}$ ions results in a distortion of the $V_2O_5$ lattice. This distortion is more important with tungsten and the solid solution obtained in that case is limited to 7 mole% $WO_3$ while for $MoO_3$ it goes up to 15% at room temperature. ESR experiments performed on $Mo^{6+}$-doped $V_2O_5$ single crystals (*14*) show that the charge difference is compensated on a local range, the unpaired electron being localized on a $V^{4+}$ ion near the $Mo^{6+}$. These results were then extended to $W_xV_2O_5$ (*5*) but no detailed ESR study has been yet published.

In this paper, we present an ESR study of $W_xV_2O_5$ single crystals, up to the solid solution limit, in order to get more information about the nature of the paramagnetic defects. Such defects take an important part in the semiconducting properties of the oxide as well as in its catalytic activity toward oxidation reactions.

## Experimental

Solid solutions of $WO_3$–$V_2O_5$ were made

0022-4596/80/090335-05$02.00/0

TABLE I

UNIT-CELL PARAMETERS OF AN ORTHORHOMBIC $V_2O_5$–$WO_3$ SOLID SOLUTION

| Mole% of $WO_3$ | $a$ (Å) | $b$ (Å) | $c$ (Å) |
|---|---|---|---|
| 0 | 11.510 | 4.370 | 3.563 |
| 3 | 11.518 | 4.350 | 3.564 |
| 7 | 11.524 | 4.340 | 3.565 |

by melting together the two oxides in the appropriate ratio. Single crystals were grown by zone melting in an image furnace. Crystals of 5 × 2 × 0.5 $mm^3$ were obtained and easily cleaved along the *ac* plane. X-Ray diffraction of powders was performed on a Philips diffractometer, using Cu $K\alpha$ radiation. ESR experiments were made on an X-band spectrometer (JEOL ME3X); all spectra presented in this paper were recorded at low temperature (−130°C) by blowing cold nitrogen gas through the cavity. Accurate measurements of the magnetic field were made with an NMR proton probe.

## Results

X-Ray experiments show that $WO_3$ gives orthorhombic solid solutions with $V_2O_5$ up to 7 mole% of $WO_3$. Table I gives the measured lattice parameters. It shows that $a$ and $c$ slightly increase with tungsten content while $b$ decreases.

A typical low-temperature ESR spectrum of $W_xV_2O_5$ single crystal ($x = 0.005$) is shown in Fig. 1. It exhibits the eight hyperfine lines due to an unpaired electron localized on a $V^{4+}$ ion ($I = 7/2, S = 1/2$). The hyperfine structure remains resolved in all directions, the best spectrum being obtained along the *b* direction. The spectrum is almost isotropic in the *ac* plane and anisotropic outside this plane, indicating a $V^{4+}$ ion in a crystal field strongly distorted along the *b* axis. This corresponds to the site symmetry around vanadium in the $V_2O_5$ lattice (Fig. 2).

Table II gives the ESR parameters measured for pure $V_2O_5$ and $W_xV_2O_5$ ($x = 0.005$) single crystals, along with those obtained by Boesman and Gillis (*14*) for $Mo_xV_2O_5$ ($x = 0.005$).

As for $Mo_xV_2O_5$ (*14*) the eight-line pattern is conserved when the sample is ro-

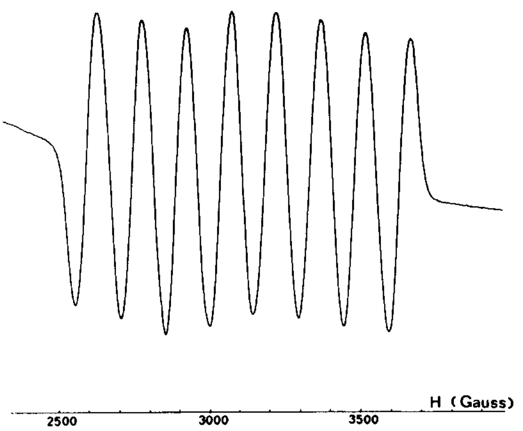

FIG. 1. ESR spectrum of $W_xV_2O_5$ single crystal ($x = 0.005$). The magnetic field is parallel to the **b** axis. Recording temperature: −130°C.

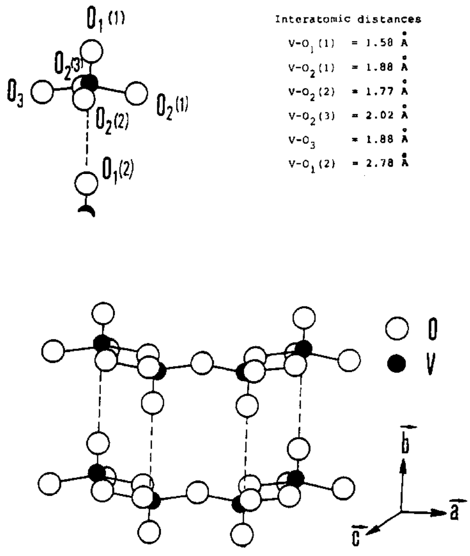

FIG. 2. Site symmetry and V–O distances in $V_2O_5$ according to Ref. (*15*).

tated about the *a* and *b* axes. The angular variation is much more complicated when the magnetic field is rotating about the *c* axis, in the *ab* plane. For $\widehat{Ha}$ or $\widehat{Hb} \neq 0$, the low- and high-field lines are split and a complicated spectrum is observed (Fig. 3). This splitting is more visible on the high-field side of the spectrum. It may correspond to the superposition of two eight-line spectra incompletely resolved because of the large linewidth ($\Delta H \simeq 80$ G). The ESR spectra of $V_2O_5$–$WO_3$ solid solutions, up to 7 mole% of $WO_3$, remain almost unchanged. The linewidth increases, but this is probably due to the valence induction effect (*9*). The $V^{4+}$ ratio increases with $x$ and the mean distance between paramagnetic defects decreases, leading to a dipolar broadening of the ESR spectrum. Table III gives the evolution of the ESR parameters up to 7 mole% of $WO_3$. The $g_b$ value slightly decreases ($g_b = 1.8831$ for $x = 0.05$) when $WO_3$ is added.

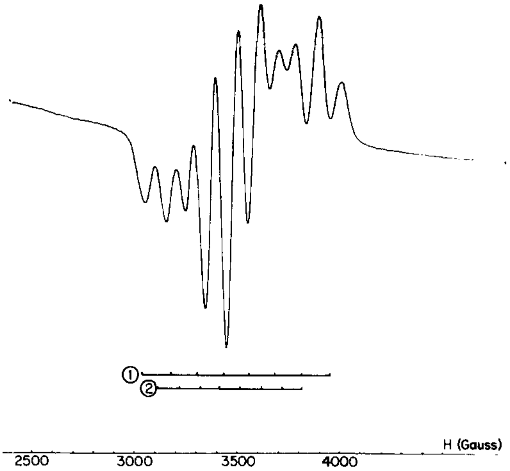

FIG. 3. Low-temperature ESR spectrum of a $W_xV_2O_5$ crystal ($x = 0.005$) when $H$ is perpendicular to c, and $\widehat{Hb} = 60°$.

## Discussion

### (a) Nature of the Defect and Lattice Distortion

The anisotropic eight-line ESR spectrum observed in Fig. 1 is typical of a $V^{4+}$ ion in an axially distorted crystal field. This means that the unpaired electron in $W_xV_2O_5$ is localized on a single vanadium instead of two as in pure $V_2O_5$. Such a modification of the defect is observable even for very low concentrations of tungsten, down to 0.1 mole% of $WO_3$. It has been postulated (*14*) that the unpaired electron, attracted by the positive charge of $W^{6+}$, is trapped on a vanadium site near the tungsten, leading to defects like $W^{6+}$–O–$V^{4+}$.

According to the structure of orthorhombic $V_2O_5$ (*15*), a $W^{6+}$ occupying a vanadium site may have four different vanadium neighbors. Three of them are directed along the *a*, *b*, or *c* directions (Fig. 2). The fourth corresponds to the shortest V–V distance

TABLE II

ESR PARAMETERS FOR PURE AND DOPED $V_2O_5$ SINGLE CRYSTALS[a]

| | $g_a$ | $g_b$ | $g_c$ | $A_a$ (G) | $A_b$ (G) | $A_c$ (G) |
|---|---|---|---|---|---|---|
| $V_2O_5$ | 1.9803 | 1.9131 | 1.9803 | 33 | 88 | 33 |
| $Mo_xV_2O_5$ | 1.981 | 1.905 | 1.977 | 52.8 | 158.5 | 50.8 |
| $W_xV_2O_5$ | 1.9807 | 1.8866 | 1.9801 | 54.4 | 161 | 51.4 |

[a] $V_2O_5$ and $W_xV_2O_5$ measurements were made in our laboratory while for $Mo_xV_2O_5$ they are taken from Boesman and Gillis (*14*).

TABLE III

ESR PARAMETERS OF $W_xV_2O_5$ SINGLE CRYSTALS

| Mole% of $WO_3$ | $g_\parallel$ | $g_\perp$ | $A_\parallel$ (G) | $A_\perp$ (G) |
|---|---|---|---|---|
| 0 | 1.9131 | 1.9803 | 88 | 33 |
| 0.5 | 1.8866 | 1.9804 | 161 | 53 |
| 1 | 1.885 | 1.979 | 162.5 | 54 |
| 5 | 1.882 | 1.984 | 167 | Not resolved |

[a] The parallel direction is taken along the *b* axis: $g_\parallel = g_b$ and $g_\perp = \frac{1}{2}(g_a + g_c)$.

(3.09 Å). If we compare the ESR spectra obtained with pure and doped $V_2O_5$, apart from the number of hyperfine lines, the main variation concerns the $g_b$ value which decreases noticeably from pure $V_2O_5$ to $Mo_xV_2O_5$ and $W_xV_2O_5$. This leads us to think that the $W^{6+}$–O–$V^{4+}$ defect is directed along the *b* axis. This model corresponds with one of those proposed by Boesman and Gillis (*14*) for Mo-doped $V_2O_5$, but here, the $g_b$ shift is much more important than in their case. It agrees also with the tendency of $W^{6+}$ ions toward octahedral coordination which can be achieved here by displacing the oxygen ion lying between $W^{6+}$ and $V^{4+}$.

According to ESR results, these $V^{4+}$ ions are in an orthorhombic crystal field but $g_a$ and $g_c$ are so close that we can approximate the site symmetry to $C_{4v}$, the $C_4$ axis lying along *b*. We then have $g_\parallel = g_b$ and $g_\perp = g_a = g_c$. Table II shows that the difference $(g_\perp - g_\parallel)$ increases from pure $V_2O_5$ (0.067) to $Mo_xV_2O_5$ (0.076) and $W_xV_2O_5$ (0.094). This could be related to the lattice deformation which has been observed by NMR (*13*), the distortion being more important with $W^{6+}$ than with $Mo^{6+}$. Anyway, it is noticeable that only $g_\parallel$ is modified while $g_\perp$ remains almost constant.

The crystal field around the $V^{4+}$ ion has $C_{4v}$ symmetry. The unpaired electron lies in a $3d_{xy}$ orbital and we can write (*16*) (Fig. 4)

$$g_\parallel = g_e - \frac{8\lambda}{\Delta E(b_1 - b_2)},$$

$$g_\perp = g_e - \frac{2\lambda}{\Delta E(e - b_2)}.$$

The decrease of $g_\parallel$ when adding $M^{6+}$ indicates a decrease of the energy gap between the $d_{x^2-y^2}$ and $d_{xy}$ levels. These orbitals are involved in the V–O bonds in the *ac* plane. A modification of these bonds is then observed. This agrees with the X-ray data (Table I) showing a variation of the *a* and *c* parameters. The $g_\perp$ value on the other hand does not vary. It involves mainly the $d_{xz}$ and $d_{yz}$ orbitals which give the $\pi$ bonding in the short V=O double bond along the *b* axis. This bond does not seem to be altered much when adding Mo or W.

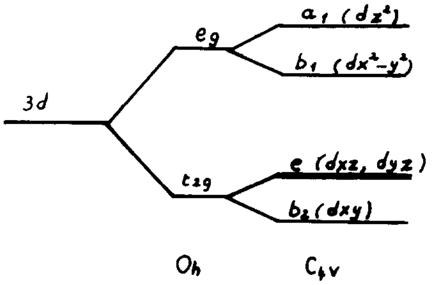

FIG. 4. Crystal field splitting of 3*d* orbitals in $C_{4v}$ site symmetry. According to LCAO *MO* theory, $b_2$, *e*, $b_1$, and $a_1$ correspond to the antibonding molecular orbitals which are mainly of metallic character (*16*).

We may then suggest the following model for the paramagnetic defects in $W_xV_2O_5$. At low temperature, the unpaired electron is trapped on a single vanadium, near the $W^{6+}$ in the *b* direction. The $V^{4+}$ ion thus formed would have its short $V{=}O_{1(1)}$ bond opposite to $W^{6+}$ while the weak $V{-}O_{1(2)}$ bond would be directed toward the tungsten, so that the oxygen lying between $V^{4+}$ and $W^{6+}$ could be easily shifted along the *b* axis (Fig. 5).

### (*b*) *Vanadium Shift in the Defect*

The angular variation of the ESR spectrum when the magnetic field is rotated in the *ab* plane about the *c* axis, indicates that we are dealing with a set of two magnetically nonequivalent defects. These defects appear equivalent in some orientations, especially along the *a*, *b*, and *c* axes, but different for any orientation perpendicular to *c*, except *a* and *b*.

This behavior could be explained by a slight shift of the $V^{4+}$ ion along the *a* direction. In all the compounds where a V=O double bond is observed, the main axis of the *g* tensor usually corresponds to the V=O direction. We may then think that

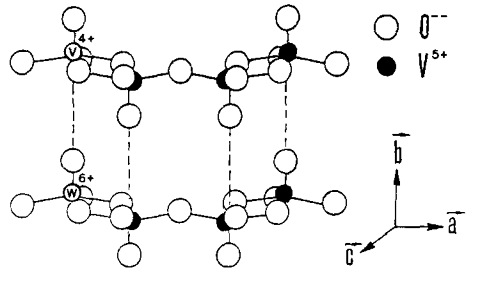

FIG. 5. Proposed model of a paramagnetic defect in $\alpha$-$W_xV_2O_5$.

in our case the V=O bond is not directed along the *b* axis but makes an angle $\alpha$ with it. Such a shift may correspond to the tendency of $V^{4+}$ toward octahedral coordination. It has been observed, in vanadium bronzes where both $V^{4+}$ and $V^{5+}$ ions are present, that $V^{4+}$ occupies the octahedral sites, while $V^{5+}$ enters in the distorted sites (*17*). If such a process arose here, $V^{4+}$ ions would tend to come nearer to the $O_3$ oxygen in the *ac* plane (Fig. 2).

According to the $V_2O_5$ structure, half of the $V^{4+}$ ions would be shifted in one direction along **a** and half of them in the opposite direction. We should then have two sets of paramagnetic defects characterized by the same *g* and *A* values but with their main magnetic axis ($V$–$O_{1(1)}$) making an angle ± $\alpha$ with **b** in the *ab* plane. Such defects would be equivalent for any direction of the magnetic field in the *bc* and *ac* planes. They would not be equivalent in the *ab* plane between the *a* and *b* axes. A computer simulation based on this model shows that one can fit reasonably well the observed spectrum if $\alpha = 4°$. Taking this value, we may estimate the $V^{4+}$ shift in the *a* direction. A straightforward calculation gives 0.08 Å. Table IV gives a comparison of the V–O distances for $V^{5+}$ and $V^{4+}$, according to our model. It shows that the $V^{4+}$ ion lies nearer the middle of the four oxygens in the *ac* plane than the $V^{5+}$ ion.

TABLE IV

ESTIMATED $V^{4+}$ DISTANCES IN THE *ac* PLANE

| | $V^{5+}$ (Å) | $V^{4+}$ (Å) |
|---|---|---|
| $V$–$O_3$ | 2.021 | 1.941 |
| $V$–$O_{2(2)}$ | 1.878 | 1.878 |
| $V$–$O_{2(3)}$ | 1.878 | 1.878 |
| $V$–$O_{2(1)}$ | 1.780 | 1.860 |

## References

1. A. B. SCOTT, J. C. MCCULLOCH, AND K. M. MAR, "Conduction in Low-Mobility Materials," p. 105, Taylor and Francis, London (1971).
2. J. PERLSTEIN AND M. SIENKO, *J. Chem. Phys.* **48**(1), 174 (1968).
3. J. HAEMERS, E. BAETENS, AND J. VENNICK, *Phys. Status Solidi A* **20**, 381 (1973).
4. E. GILLIS AND E. BOESMAN, *Phys. Status Solidi* **14**, 337 (1966).
5. G. SPERLICH, *Z. Phys.* **250**, 335 (1972).
6. G. SPERLICH AND W. D. LAZE, *Phys. Status Solidi B* **65**, 625 (1974).
7. K. TARAMA, S. H. TERANIGHI, AND S. YOSHIDA, *Bull. Inst. Chem. Res. Kyoto Univ.* **46**, 185 (1968).
8. V. V. VOLKOV, G. S. TINCHACHEVA, A. A. FOTIOEV, AND E. V. CHACHENKO, *Zh. Neorg. Khim.* **17**, 2803 (1972).
9. E. BURZO, L. STANESCU, AND D. UNGUR, *Solid State Commun.* **18**, 537 (1976).
10. L. STANESCU AND I. ANDELEAN, *Rev. Roum. Phys.* **21**, 10, 1049 (1976).
11. L. STANESCU, E. INDREA, I. ARDELEAN, M. COLDEA, I. BRATU, AND D. STANESCU, *Rev. Roum. Phys.* **21**, 9, 939 (1976).
12. E. BURZO AND L. STANESCU, *Mater. Res. Bull.* **13**, 237 (1978).
13. M. COLDEA, L. STANESCU, AND I. ANDELEAN, *Phys. Status Solidi A* **26**, K145 (1974).
14. E. BOESMAN AND E. GILLIS, *Phys. Status Solidi* **14**, 349 (1966).
15. H. G. BACHMAN, F. R. AHMED, AND W. H. BARNES, *Z. Kristallogr.* **115**, 110 (1961).
16. C. J. BALLHAUSEN AND H. B. GRAY, *J. Inorg. Chem.* **1**(1), 111 (1962).
17. P. HAGENMULLER, *Progr. Solid State Chem.* **5**, 71 (1971).